Obesity is associated with macrophage accumulation in adipose tissue

See the related Commentary beginning on page 1785.

Stuart P. Weisberg,[1] Daniel McCann,[1] Manisha Desai,[2] Michael Rosenbaum,[1] Rudolph L. Leibel,[1,3,4] and Anthony W. Ferrante, Jr.[3,4]

[1]Division of Molecular Genetics, Department of Pediatrics,
[2]Department of Biostatistics,
[3]Deparment of Medicine, and
[4]Naomi Berrie Diabetes Center, Columbia University, New York, New York, USA

Obesity alters adipose tissue metabolic and endocrine function and leads to an increased release of fatty acids, hormones, and proinflammatory molecules that contribute to obesity associated complications. To further characterize the changes that occur in adipose tissue with increasing adiposity, we profiled transcript expression in perigonadal adipose tissue from groups of mice in which adiposity varied due to sex, diet, and the obesity-related mutations *agouti* (A^y) and *obese* (Lep^{ob}). We found that the expression of 1,304 transcripts correlated significantly with body mass. Of the 100 most significantly correlated genes, 30% encoded proteins that are characteristic of macrophages and are positively correlated with body mass. Immunohistochemical analysis of perigonadal, perirenal, mesenteric, and subcutaneous adipose tissue revealed that the percentage of cells expressing the macrophage marker F4/80 (F4/80$^+$) was significantly and positively correlated with both adipocyte size and body mass. Similar relationships were found in human subcutaneous adipose tissue stained for the macrophage antigen CD68. Bone marrow transplant studies and quantitation of macrophage number in adipose tissue from macrophage-deficient ($Csf1^{op/op}$) mice suggest that these F4/80$^+$ cells are CSF-1 dependent, bone marrow–derived adipose tissue macrophages. Expression analysis of macrophage and nonmacrophage cell populations isolated from adipose tissue demonstrates that adipose tissue macrophages are responsible for almost all adipose tissue TNF-α expression and significant amounts of iNOS and IL-6 expression. Adipose tissue macrophage numbers increase in obesity and participate in inflammatory pathways that are activated in adipose tissues of obese individuals.

J. Clin. Invest. **112**:1796–1808 (2003). doi:10.1172/JCI200319246.

Introduction

Adiposity, the fraction of total body mass comprised of neutral lipid stored in adipose tissue, is closely correlated with important physiological parameters such as blood pressure, systemic insulin sensitivity, and serum triglyceride and leptin concentrations (1–3). Strong positive correlations exist between degree of adiposity and several obesity-associated disorders such as hypertension, dyslipidemia, and glucose intolerance (2, 4). Visceral fat mass is more closely correlated with obesity-associated pathology than overall adiposity (5, 6). Obesity in humans is an independent risk factor for myocardial infarction, stroke, type 2 diabetes mellitus, and certain cancers (7–9).

Changes in adipose tissue mass are associated with changes in the endocrine and metabolic functions of adipose tissue that link increased adiposity to alterations in systemic physiology. Increased adipocyte volume and number are positively correlated with leptin production, and leptin is an important regulator of energy intake and storage, insulin sensitivity, and metabolic rate (10–13). Leptin signaling has also been implicated in the pathogenesis of arterial thrombosis (14). Adiposity is negatively correlated with production of adiponectin (also known as ACRP30), a hormone that decreases hepatic gluconeogenesis and increases lipid oxidation in muscle (15–17).

The altered production of proinflammatory molecules (so-called "adipokines") by adipose tissue has been implicated in the metabolic complications of obesity. Compared with adipose tissue of lean individuals, adipose tissue of the obese expresses increased amounts of proinflammatory proteins such as TNF-α, IL-6, iNOS (also known as NOS2), TGF-β1, C-reactive protein, soluble ICAM, and monocyte chemotactic protein-1 (MCP-1) (18–25), and procoagulant proteins such as plasminogen activator

Received for publication June 19, 2003, and accepted in revised form October 13, 2003.

Address correspondence to: Anthony W. Ferrante, Jr., Naomi Berrie Diabetes Center, Columbia University, 1150 St. Nicholas Avenue, New York, New York 10032, USA. Phone: (212) 851-5322; Fax: (212) 851-5331; E-mail: awf7@columbia.edu.

Conflict of interest: The authors have declared that no conflict of interest exists.

Nonstandard abbreviations used: monocyte chemotactic protein-1 (MCP-1); plasminogen activator inhibitor type 1 (PAI-1); stromal vascular cell (SVC); diet-induced obese (DIO); fatty acid–poor BSA (FAP-BSA); *colony-stimulating factor 1 receptor (Csf1r)*; thiazolidinedione (TZD).

inhibitor type-1 (PAI-1), tissue factor, and factor VII (26–28). Obese mice deficient in TNF-α and iNOS are more sensitive to insulin than are obese wild-type mice (21, 29). Proinflammatory molecules have direct effects on cellular metabolism. For example, TNF-α directly decreases insulin sensitivity and increases lipolysis in adipocytes (30, 31). IL-6 leads to hypertriglyceridemia in vivo by stimulating lipolysis and hepatic triglyceride secretion (32).

Despite the increased production of proinflammatory molecules, infiltration of adipose tissue by inflammatory cells has not been described as a common feature of obesity. That adipocytes express receptors for several proinflammatory molecules (e.g., TNF-α, IL-6) supports models in which adipocytes were both the source and target of proinflammatory signals. However, recent data suggest that in adipose tissue, proinflammatory molecules, including IL-1β, PG-E2, TNF-α, and IL-6, are produced by stromal vascular cells (SVCs) (33, 34).

To identify genes whose expression correlated with adiposity, we profiled gene expression in perigonadal adipose tissue from 24 mice in which adiposity varied due to sex, diet, and the obesity-related mutations *agouti* (A^y) and *obese* (Lep^{ob}).We used an analytical approach that calculated Kendall's τ, a nonparametric, robust correlation statistic for each gene in our data set. This analysis identified 1,304 transcripts that were significantly correlated with body mass, an easily measured indirect indicator of adiposity. A large proportion of these transcripts encoded proteins characteristic of macrophages. These results suggested — and histological data from both mice and humans confirmed — that the macrophage content of adipose tissue correlated positively with two indices of adiposity: BMI and adipocyte size. Expression analysis of macrophage and nonmacrophage cell populations isolated from adipose tissue showed that adipose tissue macrophages are the primary sources of TNF-α and other proinflammatory molecules in adipose tissue.

Methods

Animals and animal care. Unless otherwise noted, all mice were obtained from The Jackson Laboratory (Bar Harbor, Maine, USA) at 6–8 weeks of age and housed in ventilated Plexiglas cages (one to three animals per cage) within a pathogen-free barrier facility that maintained a 12-hour light/dark cycle. Mice had free access to autoclaved water and irradiated pellet food. C57BL/6J mice in which obesity was induced by a high-fat diet (diet-induced obese or DIO mice) were fed pellets that derived approximately 45% of calories from lipids (diet D12451; Research Diets Inc., New Brunswick, New Jersey, USA) for 12 weeks. All other mice were fed a standard pellet diet that derived about 5% of calories from lipids (PicoLab Rodent Diet 20; Purina Mills Inc., Brentwood, Missouri, USA). The toothless FVB/NJ $Csf1^{op/op}$ mice were fed a powdered form of the standard diet.

Mice were sacrificed by CO_2 asphyxiation at 20–21 weeks of age during the second and third hour of the light cycle. Animals were weighed and adipose tissues (epididymal or parametrial, perirenal, mesenteric, and inguinal subcutaneous depots), liver, and extensor digitalis longus muscle were removed. Tissues to be analyzed by FACS were processed immediately; other samples were frozen in liquid nitrogen and stored at –75°C prior to RNA extraction and immunohistochemical analysis. All procedures were approved by Columbia University's Institutional Animal Care and Use Committee.

A total of 24 mice were included in the microarray expression study, four from each of the following groups: C57BL/6J males, C57BL/6J females, high fat–fed C57BL/6J males, B6.Cg A^y/+ females, B6.V $Lep^{ob/ob}$ males, and B6.V $Lep^{ob/ob}$ females. In B6.Cg A^y/+ mice, ectopic overexpression of the agouti transcript leads to a moderate increase in the mass of adipose tissue and a hyperleptinemic form of obesity (35). Feeding male C57BL/6J mice a high-fat diet also leads to hyperleptinemic moderate obesity. B6.V $Lep^{ob/ob}$ mice are leptin-deficient and severely obese (36, 37). A pair of 2-month-old macrophage-deficient (FVB/NJ $Csf1^{op/op}$) and control (FVB/NJ $Csf1^{+/+}$) female mice were a gift of E. Richard Stanley (Albert Einstein College of Medicine, New York, New York, USA). Macrophage-deficient mice are osteopetrotic and toothless; these mice were maintained on a powdered chow diet (~5% fat content). For transplant experiments, $CD45.2^+$ (C57BL/6J) recipient and $CD45.1^+$ (B6.SJL *Ptprca Pep3b*/BoyJ) donor mice were purchased from The Jackson Laboratory. These mice are homozygous for antigenically distinct forms of the CD45 protein, a protein expressed on all leukocytes.

Human subjects and materials. Healthy lean, overweight, and obese subjects were admitted to the Clinical Research Center at Columbia Presbyterian Medical Center (New York, New York, USA) as part of a longitudinal study of the metabolic effects of weight perturbation. The details of this study have been described previously (38–40). The study protocol was approved by the Institutional Review Board of Columbia University, and written informed consent was obtained from each subject. Subjects were fed a liquid formula diet of 40% fat (corn oil), 45% carbohydrate (glucose polymer), and 15% protein (casein hydrolysate) supplemented with 5.0 g iodized NaCl, 1.9 g K, and 2.5 g calcium carbonate per day, 1 mg of folic acid twice weekly, and 36 mg ferrous iron every other day. Daily formula intake was adjusted until weight stability — defined as a slope of < 0.01 kg/d in a 14-day plot of weight versus days — was achieved. Subjects were fed the liquid formula diet for 5–8 weeks before adipose tissue aspiration was performed. Subjects in the postabsorptive state underwent needle aspirations of abdominal subcutaneous adipose tissue at the level of the umbilicus. Local anesthesia was achieved with 1% xylocaine, and 2–4 g subcutaneous adipose tissue was aspi-

rated using a 15-gauge needle. A sample of tissue was frozen immediately in liquid nitrogen and stored at –80°C. These samples were used in the studies of tissue morphology and gene expression described here.

Microarray gene expression. Total RNA was extracted from the perigonadal (epididymal or parametrial) adipose tissue of individual mice using a commercially available acid-phenol reagent (TRIzol; Invitrogen Corp., Carlsbad, California, USA). RNA concentration was assessed by absorbance spectroscopy, and RNA integrity was confirmed by nondenaturing agarose gel electrophoresis. Twenty micrograms of RNA from each sample was further purified to remove contaminating organics and non-RNA species using a silica resin (RNeasy; Qiagen Inc., Valencia, California, USA) protocol according to the manufacturer's instructions. Total RNA from single animals was individually converted into biotinylated, fragmented cRNA using protocols recommended by the microarray manufacturer (Affymetrix Inc., Santa Clara, California, USA). Samples of cRNA derived from single animals were hybridized in recommended buffer to microarrays (Murine Genome Array U74Av2, Affymetrix Inc.) at 45°C for 16 hours. The samples were stained and washed according to the manufacturer's protocol on a Fluidics Station 400 (Affymetrix Inc.) and scanned on a GeneArray Scanner (Affymetrix Inc.). Primary data extraction was performed with Microarray Suite 5.0 (Affymetrix Inc.), and signal normalization across samples was carried out using all probe sets with a mean expression value of 500.

Statistical analyses. Without any computational prefiltering of genes, the normalized expression signal from each microarray probe set was examined to identify genes that were significantly associated with body mass among the 24 mice in this study. We used Kendall's τ statistic, a rank-based test of correlation, to detect transcripts whose expression levels were significantly correlated with body mass. Each analysis was performed by allowing the false discovery rate to be no more than 0.03, where the false discovery rate was defined as the expected proportion of falsely rejected hypotheses ("false positives") as described by Benjamini and Hochberg (41). We used a false discovery rate rather than standard significance measures to avoid an inflated false-positive rate as a consequence of the large number of hypothesis tests (42). All statistical analyses were implemented in S-Plus (http://www.insightful.com) or R (http://www.r-project.org).

Immunohistochemistry. Adipose tissue, muscle, and liver samples were fixed for 12–16 hours at room temperature in zinc-formalin fixative (Anatech Ltd., Battle Creek, Michigan, USA) and embedded in paraffin. Five-micron sections cut at 50-μm intervals were mounted on charged glass slides, deparaffinized in xylene, and stained for expression of F4/80 as described by Cecchini et al. (43) with an anti-F4/80 monoclonal antibody provided by E. Richard Stanley (Albert Einstein College of Medicine), or for expression of CD68 with the commercially available monoclonal antibody PG-M1 according to the manufacturer's instructions (Dako CytoMation, Carpinteria, California, USA). For each individual mouse adipose depot, four different high-power fields from each of four different sections were analyzed. The total number of nuclei and the number of nuclei of F4/80-expressing cells were counted for each field. The fraction of F4/80-expressing cells for each sample was calculated as the sum of the number of nuclei of F4/80-expressing cells divided by the total number of nuclei in sections of a sample. The same procedure was used to measure the fraction of CD68-expressing cells in human tissues. Adipocyte cross-sectional area was determined for each adipocyte in each field analyzed using image analysis software (SPOT version 3.3; Diagnostic Instruments Inc., Sterling Heights, Michigan, USA). Average adipocyte cross-sectional area was calculated for each animal using Microsoft Excel (Microsoft Corp., Redmond, Washington, USA).

Isolation of adipose tissue macrophages, adipocytes, and SVCs. Adipose tissue was isolated from mice immediately after CO_2 asphyxiation. Tissues were handled using sterile techniques and minced into fine (<10 mg) pieces. Minced samples were placed in HEPES-buffered DMEM (Invitrogen Corp.) supplemented with 10 mg/ml fatty acid–poor BSA (FAP-BSA; Sigma-Aldrich, St. Louis, Missouri, USA) and centrifuged at 1,000 *g* for 10 minutes at room temperature to pellet erythrocytes and other blood cells. An LPS-depleted collagenase cocktail (Liberase 3; Roche Applied Science, Indianapolis, Indiana, USA) at a concentration of 0.03 mg/ml and 50 U/ml DNase I (Sigma-Aldrich) was added to the tissue suspension and the samples were incubated at 37°C on an orbital shaker (215 Hz) for 45–60 minutes. Once digestion was complete, samples were passed through a sterile 250-μm nylon mesh (Sefar America Inc., Depew, New York, USA). The suspension was centrifuged at 1,000 *g* for 10 minutes. The pelleted cells were collected as the SVCs, and the floating cells were collected as the adipocyte-enriched fraction. The adipocyte fraction was further digested for 1 hour, washed twice with DMEM, and centrifuged as above until there was no further cell/debris pellet. The SVCs were resuspended in erythrocyte lysis buffer and incubated at room temperature for 5 minutes. The erythrocyte-depleted SVCs were centrifuged at 500 *g* for 5 minutes, and the pellet was resuspended in FACS buffer (PBS containing 5 mM EDTA and 0.2% [wt/vol] FAP-BSA).

Immunophenotyping and FACS. SVCs isolated from adipose tissue samples were cooled on ice and counted using a hemocytometer. Cell survival rates ranged from 70% to 90%. After counting the cells, we centrifuged them at 500 *g* for 5 minutes and resuspended in FACS buffer at a concentration of 7×10^6 cells/ml. Cells were incubated in the dark at 4°C on a bidirectional shaker for 30 minutes in FcBlock (20 μg/ml) (BD Pharmingen, San Jose, California, USA), then for an additional 50 minutes with fluorophore-conjugat-

ed primary antibodies or isotype control antibodies. Antibodies used in these studies included: CD11b-phycoerythrin (CD11b-PE) (2 μg/ml), CD45.1-PE (5 μg/ml), CD45.2-PE (5 μg/ml; eBioscience, San Diego, California, USA), and F4/80-APC (5 μg/ml; Caltag Laboratories Inc., Burlingame, California, USA). Following incubation with primary antibodies, 1 ml FACS buffer was added to the cells. Cells were centrifuged at 500 *g* for 5 minutes and resuspended in 1 ml FACS buffer. The wash was repeated twice. Cells were analyzed on a FACSCalibur and analysis was performed using CellQuest software (Becton, Dickinson and Co., Franklin Lakes, New Jersey, USA). Macrophages stained with F4/80-APC were separated from $F4/80^-$ cells using a FACSAria cell sorter (BD Biosciences Immunocytometry Systems Inc., San Jose, California, USA). $F4/80^+$ and $F4/80^-$ cells were collected into cooled FACS buffer, centrifuged at 500 *g* for 5 minutes, and immediately frozen for gene expression analysis.

Quantitative real-time PCR. Total RNA was extracted from frozen adipose tissue (100 mg), FACS-isolated cells (>10^5), or cultured cells (60-mm confluent plate) using a commercially available acid-phenol reagent (TRIzol; Invitrogen Corp.). For tissue samples, first-strand cDNA was synthesized using SuperScript II reverse transcriptase and random hexamer primers as described in the manufacturer's protocol (Invitrogen Corp.). Samples of cDNA were diluted 1:25 in nuclease-free water (Qiagen Inc.). For isolated cell populations, SuperScript III was used to generate cDNA. Samples from each cDNA pool were diluted 1:10, 1:30, 1:90, and 1:270 in order to create a standard curve for calculation of relative gene expression levels. PCR amplification mixtures (20 μl) contained 10 μl of 2× PCR SYBR Green I QuantiTect Master Mix (Qiagen Inc.), 0.4 μl of a mixture of 25 μM reverse and forward primers, and 11.6 μl diluted cDNA template. Real-time quantitative PCR was carried out using either the LightCycler (human samples; Roche Applied Science) or DNA Engine Opticon instruments (mouse samples; MJ Research Inc., Waltham, Massachusetts, USA) with the following cycling parameters: polymerase activation for 15 minutes at 95°C and amplification for 40 cycles of 15 seconds at 94°C, 10 seconds at 58°C, and 10 seconds at 72°C. After amplification, melting curve analysis was performed as described in the manufacturer's protocol (Qiagen Inc.). Relative expression values were calculated based on the standard curve using LightCycler software (version 3.5; Roche Applied Science).

Determination of relative expression values. The expression rates of three macrophage-specific genes (*Emr1*, *Cd68*, and *Csf1*) that correlated with body mass in our microarray studies, an adipocyte-specific gene (*Acrp30*), and proinflammatory genes (*Tnfa*, *Nos2*, *Il6*) were determined by quantitative RT-PCR. To normalize expression data, we used multiple internal control genes as described by Vandesompele et al. (44). Internal control genes were selected from our murine microarray data set and a separate human data set (A.W. Ferrante and D. McCann, unpublished results). For each species, we chose control genes with high expression levels and little sample-to-sample variability. For human controls these were *Excision repair cross-complementing group 3* (*ERCC3*), *Amplified in osteosarcoma* (*OS-9*), and *Casein kinase-1d* (*CSNK1D*). For each gene to be assayed, intron-spanning primers were designed using publicly available genomic contig sequences obtained through LocusLink (http://www.ncbi.nlm.nih.gov/LocusLink/index.html), the public domain primer design software Primer3 (http://www-genome.wi.mit.edu/genome_software/other/primer3.html), and the DNA analysis software Vector NTI Suite, version 7 (Informax Inc., Bethesda, Maryland, USA) (45). Human primer sequences were as follows: hCD68 forward (5′-GCTACATGGCGGTGGAGTACAA-3′), hCD68 reverse (5′-ATGATGAGAGGCAGCAAGATGG-3′); hERCC3 forward (5′-ACATTGACCTAAAGCCCACAGC-3′), hERCC3 reverse (5′-AGTTGCCCAGCACCAGACAG-3′); hOS-9 forward (5′-TAAACGCTACCACAGCCAGACC-3′), hOS-9 reverse (5′-AGCCGAGGAGTGCGAATG-3′); hCSNK1D forward (5′-AGGAGAAGAGGTTGCCATCAAG-3′), hCSNK1D reverse (5′-TCCATCACCATGACGTTGTAGTC-3′).

For expression analysis in mice, we used microarray data as described above to select two internal control genes, cyclophilin B (*Cphn2*) and ribosomal protein S3 (*Rps3*). Mouse primer sequences were as follows: F4/80 forward (5′-CTTTGGCTATGGGCTTCCAGTC-3′), F4/80 reverse (5′-GCAAGGAGGACAGAGTTTATCGTG-3′); CD68 forward (5′-CTTCCCACAGGCAGCACAG-3′), CD68 reverse (5′-AATGATGAGAGGCAGCAAGAGG-3′); CSF1-R forward (5′-GCATACAGCATTACAACTGGACCTACC-3′), CSF1-R reverse (5′-CAGGACATCAGAGCCATTCACAG-3′); TNF-α forward (5′-CCAGACCCTCACTAGATCA-3′), TNF-α reverse (5′ CACTTGGTGGTTTGCTACGAC-3′); IL-6 forward (5′-CCAGAGATACAAAGAAATGATGG-3′), IL-6 reverse (5′- ACTCCAGAAGACCAGAGGAAAT-3′); RPS3 forward (5′-ATCAGAGAGTTGACCGCAGTTG-3′), RPS3 reverse (5′-AATGAACCGAAGCACACCATAG-3′); iNOS forward (5′-AATCTTGGAGCGAGTTGTGG-3′), iNOS reverse (5′-CAGGAAGTAGGTGAGGGCTTG-3′); PEX11a forward (5′-GACTTTTCAGAGCCACTCAGCAC-3′), PEX11a reverse (5′-GCCCACCTTTGCCATTTCTC-3′); ACRP30 forward (5′-GCTCCTGCTTTGGTCCCTCCAC-3′), ACRP30 reverse (5′-GCCCTTCAGCTCCTGTCATTCC-3′).

For each cDNA and standard curve sample, quantitative PCR reactions were performed to assay the expression of each internal control gene. To verify that the relative expression values of the control genes provided an accurate reflection of cDNA loading, we correlated the relative expression values of the control genes with one another and with the geometric mean of the three values. The Pearson correlation coefficients were consistently greater than or equal to 0.97, strongly suggesting that expression of the three control genes provided a reasonably accurate reflection of cDNA loading. To calculate the normalized relative expression levels of each gene assayed in each sample, we divided the relative gene expression value for that sample by the geometric mean

of the relative expression values of the control genes. Separate analyses in which relative expression values were normalized with the relative expression values of each control gene yielded similar results.

Adipocyte differentiation of preadipocytes. 3T3-L1 preadipocytes (American Type Culture Collection, Manassas, Virginia, USA) were grown to confluence in DMEM-FBS at 37°C in a 5% CO_2 incubator. Two days after reaching confluence (day 0), the culture medium was changed to DMEM-FBS supplemented with insulin (50 μg/ml), 3-isobutyl-1-methylxanthine (0.4 mM), and dexamethasone (1 μM). After 2 days, the medium was again changed to DMEM-FBS supplemented with insulin (50 μg/ml). Finally, 3 days later, the medium was changed to DMEM-FBS. Medium was replaced with fresh DMEM-FBS every 3 days thereafter.

Bone marrow transplantation. Six-week-old male CD45.2$^+$ (C57BL/6J) recipient mice and syngeneic CD45.1$^+$ (B6.SJL *Ptprca Pep3b*/BoyJ) donor mice were purchased from The Jackson Laboratory. At 8 weeks of age, recipient mice received a dose of 12 Gy from a Cs^{137} source (Gammacell-40; Atomic Energy of Canada Ltd., Mississauga, Ontario, Canada). The γ radiation was administered as two 6-Gy doses separated by a 3- to 4-hour interval in order to minimize radiation toxicity. Bone marrow was collected from the femurs and tibias of sex-matched donor mice into HBSS. Donor marrow cells (5×10^6) were injected into the recipient's lateral tail vein 4 hours after irradiation. The recipient mice were maintained in a pathogen-free facility and were fed a standard chow diet and water supplemented with 0.5 ml/l of 10% Baytril (Bayer Corp., Shawnee Mission, Kansas, USA). After 4 weeks, blood was collected from recipient mice and peripheral engraftment was confirmed via FACS analysis based on presence of the CD45.1 antigen and absence of the CD45.2 antigen. Ninety-five percent of mice survived transplant and more than 95% of peripheral blood leukocytes in recipients were donor-derived CD45.1$^+$ cells. Once engraftment was confirmed, recipient mice were placed on a high-fat diet containing about 60% of calories from lipids (D12492; Research Diets Inc.) for 6 weeks. Mice were sacrificed by CO_2 asphyxiation, and SVCs from perigonadal adipose tissue were collected for FACS analysis.

Results

We hypothesized that in adipose tissue, molecular processes regulate and respond to changes in adipose tissue mass independent of diet, sex, or the mechanism of obesity. To identify transcriptional patterns that correlate with body mass, we used oligonucleotide microarrays to catalogue gene expression levels in the parametrial or epididymal adipose tissue from two dozen mice whose body mass and adiposity varied due to diet, sex, and mutations in genes affecting energy homeostasis. We examined six experimental groups of 20-week-old C57BL/6J mice: (a) lean C57BL/6J female mice, (b) lean C57BL/6J male mice, (c) moderately obese C57BL/6J male mice with diet-induced obesity, (d) moderately obese female B6.Cg $A^y/+$ mice, (e) severely obese female B6.V $Lep^{ob/ob}$ mice, and (f) severely obese male B6.V $Lep^{ob/ob}$ mice. Each group contained four mice. As expected, body mass varied widely, with a range of 19.4–68.4 g and a mean of 44.6 ± 17.9 g.

For each transcript represented on the array, we computed Kendall's τ rank-based correlation statistic as a measure of the correlation between the expression data and body mass for the entire sample of mice. To avoid potential problems of non-normality and sensitivity to outliers, we chose this nonparametric approach over the standard Pearson correlation coefficient (46). The *P* values corresponding to each test of correlation were computed exactly. With this approach, we identified 1,304 transcripts that were significantly correlated with body mass after controlling the false discovery rate at no more than 0.03. Supplemental Table 1 available online (http://www.jci.org/cgi/content/full/112/12/1796/DC1) lists all transcripts whose expression in perigonadal adipose tissue correlated with body mass.

We annotated each transcript whose expression correlated with body mass using the Gene Ontology Con-

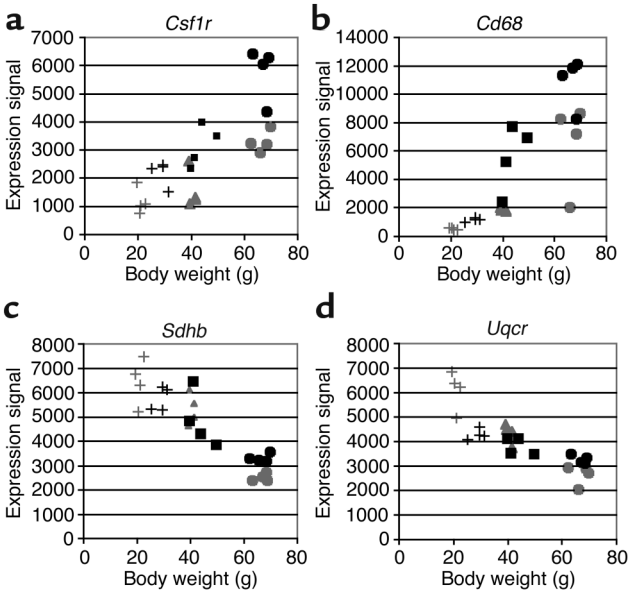

Figure 1
Adipose tissue transcripts whose abundance was correlated with body mass in mice. The expression of more than 12,000 transcripts in parametrial and epididymal adipose tissue was monitored in C57BL/6J mice whose body mass varied secondary to sex, diet, or mutations in the *agouti* ($A^y/+$) or *leptin* ($Lep^{ob/ob}$) loci. Using Kendall's τ, a nonparametric correlation metric, we identified 1,304 transcripts that correlated significantly with body mass when the false discovery rate was held to 0.03. Examples of adipose tissue transcripts whose expression correlated with body mass include (**a**) *Csf1r* and (**b**) CD68 antigen (*Cd68*), which correlated positively with body mass, (**c**) succinate dehydrogenase complex, subunit B, iron sulfur (Ip) (*Sdhb*), and (**d**) ubiquinol–cytochrome *c* reductase subunit (*Uqcr*), which correlated negatively with body mass. Gray and black symbols denote female and male mice, respectively. +, lean; triangles, $A^y/+$; squares, DIO; circles, $Lep^{ob/ob}$ mice.

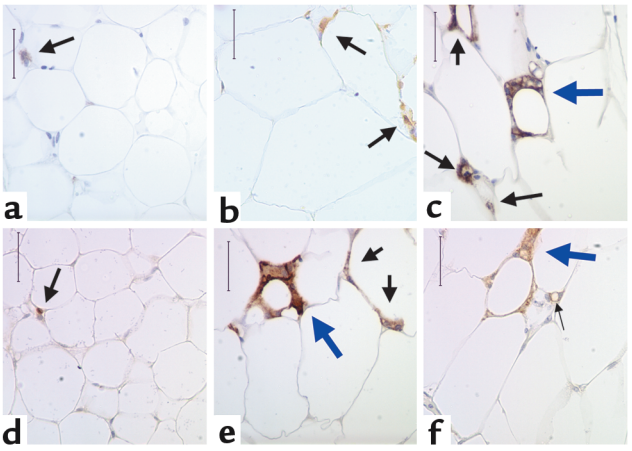

Figure 2
Adipose tissue macrophages in mice with varying degrees of adiposity. Immunohistochemical detection of the macrophage-specific antigen F4/80 (black arrows) in perigonadal adipose tissue from C57BL/6J mice: (**a**) lean female, (**b**) A^y/+ female, (**c**) $Lep^{ob/ob}$ female, (**d**) lean male, (**e**) DIO male, and (**f**) $Lep^{ob/ob}$ male. Macrophages are stained brown. In lean animals (**a** and **d**), F4/80-expressing cells were uniformly small, dispersed, and rarely seen in aggregates. The fraction of F4/80-expressing cells was greater in moderately obese mice (**b** and **e**) and greatest in the severely obese $Lep^{ob/ob}$ mice (**c** and **f**). Depots from all animals contained small, isolated F4/80 expressing cells (black arrows). In addition, depots from obese animals contained aggregates of F4/80 expressing cells (large blue arrows). Some macrophage aggregates contained small lipid-like droplets (small thin black arrow). Calibration mark = 40 μm.

sortium (http://www.geneontology.org/) and Mouse Genomics Informatics (MGI) (http://www.informatics.jax.org/) databases. Analysis of the 100 transcripts that correlated most closely with body mass (i.e., had the lowest *P* values) revealed three groups of functionally related genes that were coordinately regulated. Thirty percent of the 100 most significantly correlated transcripts encoded proteins characteristically expressed by macrophages, such as the CSF-1 receptor (τ statistic = 0.60, $P = 4.5 \times 10^{-5}$) and the CD68 antigen (τ statistic = 0.75, $P = 2.9 \times 10^{-7}$). Twelve percent encoded mitochondrial proteins such as succinate dehydrogenase complex, subunit B, iron sulfur (Ip) (τ statistic = –0.76, $P = 2.2 \times 10^{-7}$), and ubiquinol–cytochrome *c* reductase subunit (τ statistic = –0.65, $P = 7.4 \times 10^{-6}$) (Figure 1), and 6% encoded lysosomal proteins (Supplemental Table 2, http://www.jci.org/cgi/content/full/112/12/1796/DC1). The expression of all of the macrophage and lysosomal transcripts correlated positively with body mass, while the expression of each mitochondrial transcript was negatively correlated with body mass. Using quantitative RT-PCR we confirmed the expression profile of five genes (*colony-stimulating factor 1 receptor* [*Csf1r*], *Cd68*, *Pex11a*, *Emr1*, and *Mcp1*) in each of the 24 samples and found excellent agreement between the microarray and RT-PCR expression data (mean Pearson correlation coefficient = 0.91, microarray versus RT-PCR expression; Supplemental Table 3, http://www.jci.org/cgi/content/full/112/12/1796/DC1). The correlation of body mass with the expression of multiple genes characteristic of macrophages suggested that the macrophage content of adipose tissue was positively correlated with adiposity. To identify and quantitate macrophages within adipose tissue, we immunohistochemically stained sections for the F4/80 antigen, a marker specific for mature macrophages (Figure 2; ref. 43). We calculated the average adipocyte cross-sectional area and the percentage of F4/80-expressing cells in the perigonadal, perirenal, mesenteric, and subcutaneous inguinal adipose tissue depots from A^y/+ female, $Lep^{ob/ob}$ female, lean male, and diet-induced obese (DIO) male mice.

We examined the relationship between average adipocyte cross-sectional area and the percentage of adipose tissue cells expressing F4/80. Average adipocyte cross-sectional area (Figure 3) was a strong predictor of the percentage of F4/80-expressing cells for each depot. Body mass was also a strong predictor of the percentage of F4/80-expressing cells for each depot (data not shown). The regression coefficients or slopes that describe the linear relationship between average adipocyte cross-sectional area and percentage of F4/80-

Table 1
Correlation of percentage of F4/80-expressing cells in adipose tissue with adipocyte size

Depot	Obesity models included	r^2	Slope	95% C.I. of slope	*P* value
Perigonadal	Lean male (*n* = 4), DIO male (*n* = 4), A^y/+ female (*n* = 4), $Lep^{ob/ob}$ female (*n* = 3)	0.76	0.0082 (0.0012)	0.0056–0.011	$<10^{-4}$
Perirenal	DIO male (*n* = 6), lean female (*n* = 3), $Lep^{ob/ob}$ female (*n* = 4)	0.73	0.0067 (0.0011)	0.0042–0.0092	$<10^{-4}$
Mesenteric	DIO male (*n* = 5), lean female (*n* = 2), $Lep^{ob/ob}$ female (*n* = 3)	0.9	0.0068 (0.0008)	0.0050–0.0080	$<10^{-4}$
Subcutaneous	DIO male (*n* = 8), lean female (*n* = 3), $Lep^{ob/ob}$ female (*n* = 3)	0.39	0.0027 (0.0009)	0.0008–0.0047	0.01

Regression coefficients defining the relationship between the percentage of F4/80-expressing cells in adipose tissue and average adipocyte cross-sectional area in mice. Data are presented as mean ± SD. C.I., 95% confidence interval.

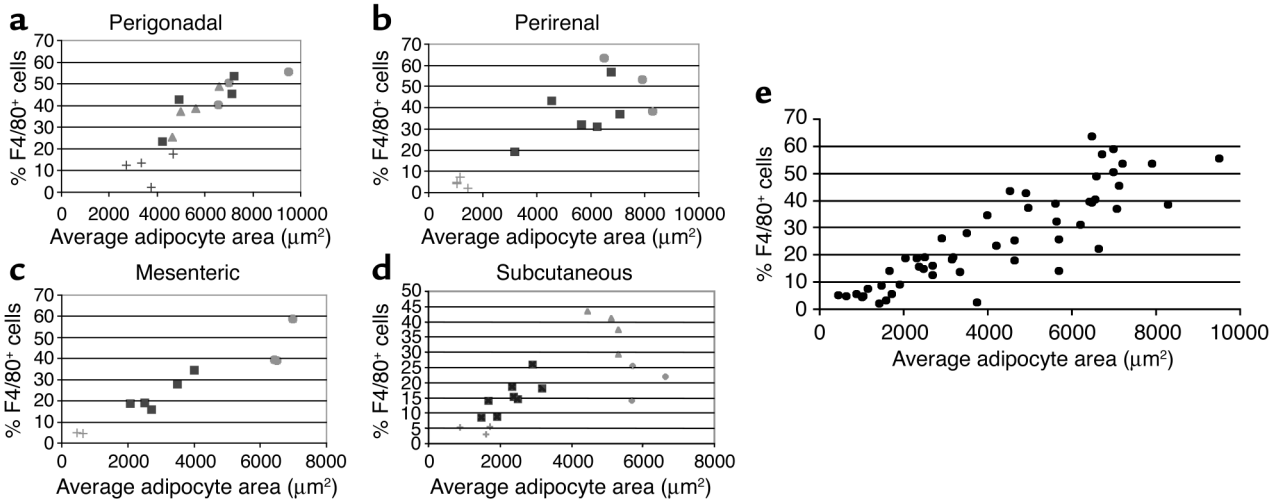

Figure 3
The relationship between adipocyte size and the percentage of macrophages in adipose tissue. Average adipocyte cross-sectional area and the percentage of F4/80$^+$ cells (macrophages) in adipose tissue depots were determined for each mouse in this study. Average adipocyte cross-sectional area was a strong predictor of the percentage of F4/80$^+$ cells in (**a**) perigonadal ($r^2 = 0.76$, $P < 10^{-4}$), (**b**) perirenal ($r^2 = 0.73$, $P < 10^{-4}$), (**c**) mesenteric ($r^2 = 0.9$, $P < 10^{-4}$), and (**d**) subcutaneous ($r^2 = 0.39$, $P < 0.01$) adipose tissue depots. (**e**) Data collected from all mice and all depots were plotted together. Light gray and dark gray symbols denote female and male mice, respectively. +, lean; triangles, $A^y/+$; squares, DIO; circles, *Lep*$^{ob/ob}$ mice.

expressing cells were comparable across mesenteric, perigonadal, and perirenal depots (Table 1). Although the slopes corresponding to adipocyte cross-sectional area for the subcutaneous depot were smaller than (and fell outside the 95% confidence intervals of) the slopes for the mesenteric and perigonadal depots, this difference was entirely attributable to the fact that the data from three B6.V *Lep*$^{ob/ob}$ mice fell below the line relating adipocyte area to macrophage content in the other animals (Table 1). Except for leptin-deficient (*ob*) subcutaneous adipose tissue, the relationship of adipose tissue macrophage accumulation to adipocyte size was similar in all depots studied (Figure 3).

Macrophages in the adipose tissue of lean mice were uniformly small, isolated, and widely dispersed among the adipocytes. In contrast, the macrophages in adipose tissue from obese animals were frequently found in aggregates. In the extremely obese animals, some of these macrophage aggregates completely surrounded adipocytes (Figure 2). These aggregates resembled the macrophage syncytia characteristic of chronic inflammatory states such as rheumatoid arthritis and foreign body giant cell induction (47–49).

We also examined the population of F4/80-expressing cells in liver and the extensor digitalis longus muscle from lean and obese *Lep*$^{ob/ob}$ female mice. In liver,

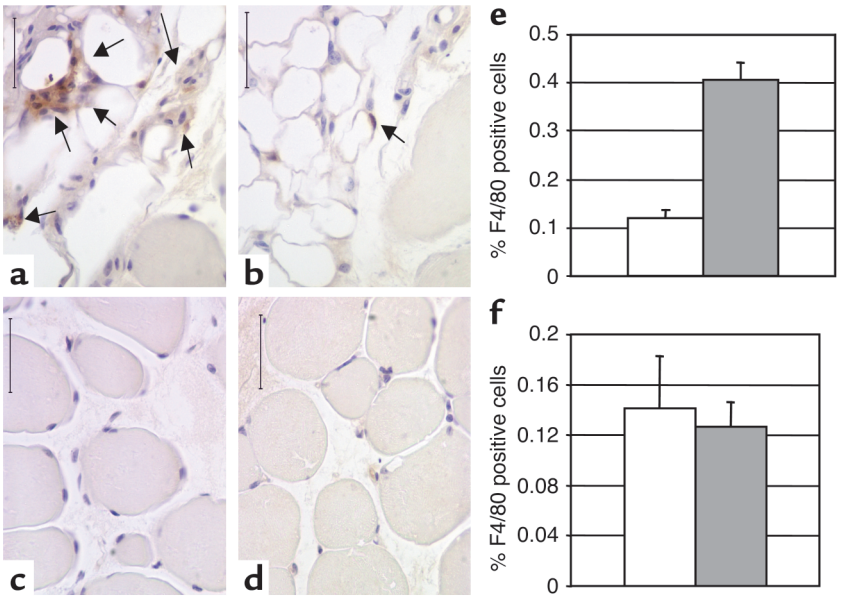

Figure 4
Macrophages in the liver and muscle of lean and obese mice. Immunohistochemical detection of cells expressing the macrophage-specific antigen F4/80 (arrows) in extensor digitalis longus muscles from C57BL/6J (**a** and **c**) *Lep*$^{ob/ob}$ female and (**b** and **d**) lean female mice. Macrophages were rarely detected in areas surrounding the myofibrils (**c** and **d**). However, muscle from both lean and obese animals was infiltrated and surrounded by adipose tissue that contained significant numbers of F4/80-positive macrophages (**a** and **b**). The percentage of F4/80-positive macrophages within this adipose tissue was markedly increased in obese compared with lean mice (**e**, $P < 0.005$). The percentage of F4/80-positive Kupffer cells within liver was not significantly altered in obesity. Calibration mark = 40 μm; white bars, lean mice; gray bars, *Lep*$^{ob/ob}$ mice.

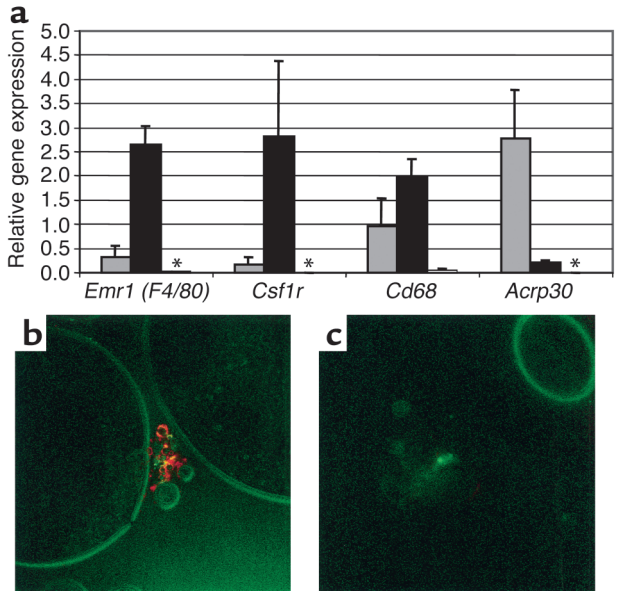

Figure 5
F4/80$^+$ cells express macrophage markers. Perigonadal adipose tissue was collected from female B6.V *Lep$^{ob/ob}$* mice, digested, and centrifuged to yield a buoyant adipocyte-enriched cell population and a pellet of SVCs. The SVCs were separated into F4/80$^+$ (black bars) and F4/80$^-$ (white bars) populations via FACS. Quantitative RT-PCR was used to measure the relative expression of macrophage markers (*Emr1*, *Csf1r*, *Cd68*) and an adipocyte-specific gene (*Acrp30*). Among the three isolated cell populations, the relative gene expression of macrophage markers was highest among the F4/80$^+$ cells. *The F4/80$^-$ SVCs did not express detectable amounts (< 0.05 of mean of all populations) of the macrophage markers. The adipocyte-enriched population (gray bars) expressed small amounts of the macrophage markers (**a**), consistent with residual macrophage contamination seen by immunofluorescent staining of live cells (**b**). In the adipocyte-enriched fraction, large autofluorescent adipocyte cell membranes (green) are not recognized by fluorescently conjugated F4/80 antibody (red), but membrane staining of small nonautofluorescent cells is seen. Control fluorescently conjugated isotype antibody did not recognize these cells (**c**).

there was no significant difference in the number of F4/80-expressing Kupffer cells between lean and obese mice (Figure 4). In muscle tissue, we observed only rare F4/80-expressing cells between myofibrils. However, muscle from both lean and obese animals was infiltrated and surrounded by adipose tissue (Figure 4). Adipose tissue within muscle contained significant numbers of F4/80$^+$ macrophages, and the percentage of F4/80$^+$ cells within this adipose tissue was markedly increased in obese mice compared with lean mice (41% ± 4% of macrophages vs. 12% ± 2% of macrophages, respectively; $P < 0.005$, mean ± SD) (Figure 4).

To more fully characterize the F4/80$^+$ cells in adipose tissue and define their cellular lineage, we used FACS to isolate and study the population of F4/80$^+$ cells from adipose tissue. Perigonadal adipose tissue was collected from obese B6.V *Lep$^{ob/ob}$* female mice and digested with a combination of collagenase I and collagenase II. The resultant digest was centrifuged and yielded a buoyant adipocyte-enriched fraction and a pellet of SVCs. The SVCs were incubated with a fluorescently labeled anti-F4/80 antibody and were sorted by FACS into F4/80-expressing (F4/80$^+$) and -nonexpressing (F4/80$^-$) populations. Quantitative RT-PCR analysis of these cell populations revealed that F4/80$^+$ cells express genes for macrophage-specific markers, including *Csf1r*, the CD68 antigen (*Cd68*), and the F4/80 antigen (*Emr1*). These are among the genes whose expression in our microarray expression data set correlated positively with body mass and adipocyte size.

The F4/80$^-$ population of cells expressed *Emr1*, *Csf1r*, and *Cd68* at less than 2% of the levels expressed in the F4/80$^+$ population (Figure 5). Using FACS we also found that all of the F4/80$^+$ cells coexpressed the common leukocyte antigen CD45 and the monocyte lineage marker CD11b (data not shown). F4/80$^+$ cells did express detectable amounts of mRNA for adiponectin/ACRP30 (*Acrp30*), albeit at levels more than an order of magnitude lower that those found in primary adipocytes and differentiated 3T3-L1 adipocytes (Figure 5). In contrast, at no timepoint during the differentiation of the preadipocyte cell line 3T3-L1 into adipocytes did we did detect significant expression of macrophage-specific genes (*Csf1r*, *Emr1*, *Cd68*) (Supplemental Table 4, http://www.jci.org/cgi/content/full/112/12/1796/DC1).

The accumulation of adipose tissue macrophages in direct proportion to adipocyte size and body mass may explain the coordinated increase in expression of genes encoding macrophage markers observed in our microarray expression data. However, macrophages and adipocytes express a number of genes in common, including *Cd36* (50), *Pparg* (51), and *aP2* (52). Preadipocytes may also have phagocytic capabilities similar to macrophages (53).

Tissue macrophages are derived from bone marrow precursors that migrate from the peripheral circulation. Preadipocyte populations are thought to be derived from resident mesenchymal cells. To test whether adipose tissue F4/80$^+$ cells shared a common bone marrow origin

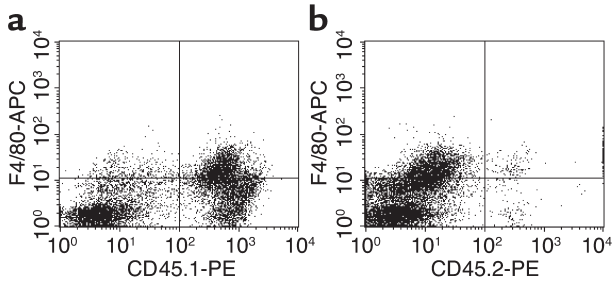

Figure 6
F4/80$^+$ cells in adipose tissue are bone marrow–derived. Adipose tissue was collected and SVCs were isolated 6 weeks after lethal irradiation and bone marrow transplantation. The SVCs were incubated with APC-conjugated anti-F4/80 (F4/80-APC and either PE-conjugated anti-CD45.1 (CD45.1-PE) or PE-conjugated anti-CD45.2 (CD45.2-PE). Eighty-five percent of F4/80$^+$ cells expressed the donor antigen, CD45.1 (right upper quadrant in **a**). Only 14% of the F4/80$^+$ cells also expressed the recipient antigen, CD45.2 (right upper quadrant in **b**).

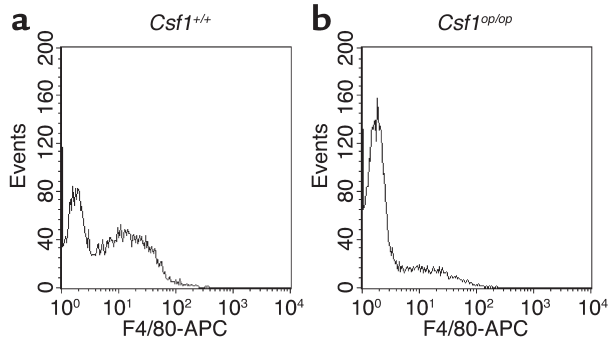

Figure 7
Macrophage-deficient FVB/NJ *Csf1*$^{op/op}$ mice are also deficient in F4/80$^+$ cells in adipose tissue. SVCs were isolated from subcutaneous and perigonadal adipose tissue of macrophage-deficient (FVB/NJ *Csf1*$^{op/op}$) and control (FVB/NJ *Csf1*$^{+/+}$) mice. Flow cytometry of SVCs isolated from two perigondadal adipose tissue depot illustrates that tissue from macrophage-deficient mice (**b**) contains 34% the number of F4/80$^+$ cells found in adipose tissue from control mice (**a**).

with other tissue macrophage populations, we transplanted bone marrow from C57BL/6J mice expressing the CD45.1 leukocyte marker into 6-week-old lethally irradiated C57BL/6J mice expressing the CD45.2 leukocyte marker. After 6 weeks on a high-fat diet, 85% of the F4/80$^+$ cells in periepididymal adipose tissue of the recipient mice were donor-derived (i.e., CD45.1$^+$). Conversely, only about 14% of the F4/80$^+$ cells in adipose tissue were recipient-derived CD45.2 cells (Figure 6). Thus most F4/80$^+$ cells in adipose tissue are bone marrow–derived.

The primary regulator of macrophage development and survival is CSF-1 (also known as M-CSF). Mice that carry a homozygous missense mutation in the *Csf1* gene (*Csf1*$^{op/op}$) are relatively macrophage deficient (43, 54, 55). As a consequence of tissue macrophage deficiency, these mice develop a complex recessive phenotype of osteopetrosis, central blindness, and infertility (56). This spontaneously arising mutation has been maintained on a mixed genetic background (C57BL/J × C3Heb/FeJ-a/a × CD1) but recently has been backcrossed onto the FVB/NJ strain (57).

In subcutaneous and parametrial adipose tissue, the mean adipocyte size of the FVB/NJ *Csf1*$^{op/op}$ mice (311 ± 71 μm^2) was smaller though not significantly different from that of control FVB/NJ *Csf1*$^{+/+}$ mice (476 ± 326 μm^2) (P = 0.37). However, FACS analysis showed that the fraction of F4/80$^+$ SVCs was significantly greater in adipose tissue from control mice than from macrophage-deficient mice. In the depots studied, the fraction of F4/80$^+$ cells in *Csf1*$^{op/op}$ mice was only 34% of that in *Csf1*$^{+/+}$ mice (P < 0.01) (Figure 7). Together these data suggest that the F4/80$^+$ cells identified in adipose tissue are CSF-1–dependent, bone marrow–derived adipose tissue macrophages.

In most tissues, macrophages are a significant source of proinflammatory molecules. To determine whether adipose tissue macrophages express any molecules implicated in obesity-associated complications, we isolated three cell populations from the parametrial adipose tissue of three obese B6.V *Lep*$^{ob/ob}$ mice: (a) an adipocyte-enriched population, (b) a stromal vascular macrophage F4/80$^+$ population, and (c) an F4/80$^-$ stromal vascular population. Following isolation, RNA was extracted from each population, and the expression of three proinflammatory genes (*Tnfa*, *Nos2*, and *Il6*) was determined by quantitative RT-PCR. Of the three adipose tissue cell populations, the F4/80$^+$ adipose tissue macrophages were the predominant source of TNF-α expression. Expression of iNOS was detectable at significant levels in each fraction, though it was highest in the macrophage fraction and thus it is likely that a significant portion of the iNOS expression in adipose tissue is derived from macrophages. In contrast, IL-6 was highly expressed in all three factions (Figure 8).

Based on these results in mice, we assessed the relationship of BMI and adipocyte size to macrophage abundance in abdominal subcutaneous adipose tissue of humans. Using quantitative RT-PCR we determined the relative expression levels of the macrophage expressed gene *Cd68* in human abdominal subcutaneous adipose tissue. We found that both BMI (r^2 = 0.43, P < 0.01; Figure 9) and average adipocyte cross-sectional area (r^2 = 0.46, P < 0.05; data not shown) were significant predictors of *Cd68* expression. *Cd68* expression was also significantly higher in the obese (BMI > 30 kg/m^2; *Cd68* expression = 1.67 ± 0.93 arbitrary units) compared to the lean subjects (BMI < 30 kg/m^2; *Cd68* expression = 0.69 ± 0.39 arbitrary units, P < 0.02).

Using an antibody that recognizes the CD68 antigen we performed immunohistochemical analysis on these human samples and calculated the percentage of

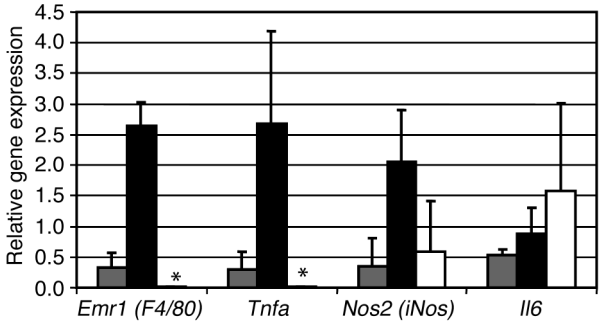

Figure 8
Adipose tissue macrophages express proinflammatory factors. Perigonadal adipose tissue was collected from female B6.V *Lep*$^{ob/ob}$ mice, digested, and centrifuged to yield a buoyant adipocyte-enriched cell population (gray bars) and a pellet of SVCs. The SVCs were separated into F4/80$^+$ macrophages (black bars) and F4/80$^-$ populations (white bars) via FACS. Quantitative RT-PCR was used to measure the relative expression of three proinflammatory genes (*Tnfa*, *Nos2*, and *Il6*). Expression of *Tnfa* was limited almost exclusively to adipose tissue macrophages. F4/80$^-$ SVCs did not express detectable amounts of *F4/80* or *Tnfa* (as indicated by asterisks). The adipocyte-enriched fractions expressed *Tnfa* at levels commensurate *F4/80* expression and consistent with macrophage contamination. *Nos2* was expressed by both macrophages and F4/80$^-$ SVCs, and *Il6* was detectably expressed by all three populations in adipose tissue.

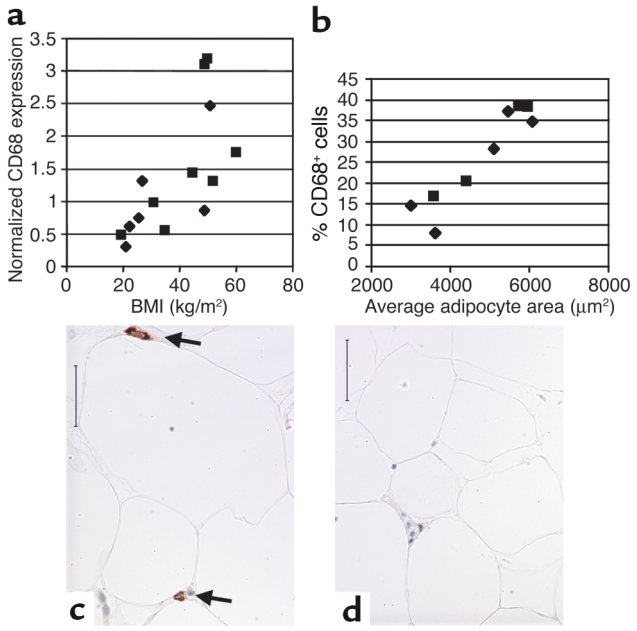

Figure 9
CD68 expression in human subcutaneous adipose tissue. Subcutaneous adipose tissue samples were aspirated from the subcutaneous abdominal region of human subjects whose BMIs ranged from 19.4 to 60.1 kg/m^2. CD68 transcript expression was measured by quantitative real-time PCR. (**a**) BMI was a significant predictor of CD68 transcript expression (r^2 = 0.43, P < 0.01). (**b**) Immunohistochemical detection and quantitation of CD68-expressing cells in subcutaneous adipose tissue from obese and lean subjects shows that the average adipocyte cross-sectional area was a strong predictor of the percentage of CD68-expressing cells (r^2 = 0.86, P < 0.001). Typical micrographs from (**c**) an obese (BMI 50.8 kg/m^2) female and (**d**) a lean (25.7 kg/m^2) female subject are shown. Arrows in **c** indicate F4/80$^+$ cells. Squares and diamonds denote female and male subjects, respectively. Calibration mark = 40 μm.

CD68 expressing cells (Figure 9). Both BMI (r^2 = 0.83, P = 0.0004; data not shown) and average adipocyte cross-sectional area (r^2 = 0.86, P = 0.0002) were strong predictors of the percentage of CD68-positive cells (Figure 9).

Discussion

Transcriptional profiling of mouse adipose tissue identified 1,304 transcripts whose expression levels were correlated with body mass in genetic and diet-induced models of obesity. Correlation of gene expression occurred across lean and obese mice, defining a common transcriptional response to variations in adiposity. These data demonstrate that variations in continuous quantitative traits such as body mass, adipocyte size, and BMI are correlated with quantitative variations in the expression of genes. Furthermore, if transcriptional regulation of adipose tissue function contributes to adiposity-dependent modulation of insulin sensitivity, blood pressure, and other medically important traits, then the genes that correlate with body mass will be candidates for mediating these responses and warrant further evaluation.

Analysis of the annotated functions of genes that correlated with body mass revealed the coordinated regulation of genes whose products are characteristic of lysosomes, mitochondria, and macrophages. Transcripts characteristic of macrophages were coordinately upregulated in direct proportion to body weight in several models of obesity. This observation suggested that the macrophage content of adipose tissue might be positively correlated with adiposity. Previous reports suggest that obesity alters the mononuclear phagocytic cell content in the circulation and within adipose tissue. Several groups have reported small increases in the numbers of circulating monocytes in severely obese individuals, and two groups have noted increased macrophage gene expression and increased numbers of phagocytic cells and cells expressing F4/80 in adipose tissue from leptin-deficient mice (58–60).

Our results indicate that adipose tissue macrophage accumulation is directly proportional to measures of adiposity in mice and humans. Immunohistochemical analysis of human subcutaneous adipose tissue showed that both BMI and adipocyte size were strong predictors of the percentage of CD68-expressing macrophages. In mice, both body mass and adipocyte size were strong predictors of the percentage of F4/80$^+$ macrophages in the perigonadal, perirenal, mesenteric, and subcutaneous adipose tissue depots. The slope that defined the linear relationship between adipocyte size and percentage of macrophages was smaller for subcutaneous adipose tissue than for the other depots. The reason for this difference is unclear. The scatterplot data suggest that macrophage accumulation in the subcutaneous depot may plateau at high degrees of adiposity, or that abnormalities associated with leptin deficiency may cause decreased macrophage accumulation specifically in the subcutaneous depot (Figure 3d). We estimate that the percentage of macrophages in adipose tissue ranges from under 10% in lean mice and humans to over 50% in extremely obese, leptin-deficient mice and nearly 40% in obese humans.

Macrophages are mononuclear phagocytes. They reside within almost all tissues, where they are identifiable as distinct populations with tissue-specific morphologies, localizations, and functions. In the liver they are Kupffer cells and line the sinusoids; in bone they form multinucleated osteoclasts at the periosteum; in the CNS they comprise the microglia, interspersed among neurons; and in the kidney they form a network around glomeruli as mesangial cells (61). Adipose tissue depots contain macrophages and macrophage precursors, but their functions have not been delineated (62, 63). In addition to tissue-specific functions, macrophages serve important immune and scavenger functions. They are the primary mediators of the innate immune response, and are important participants in adaptive immunity. They recognize and phagocytose foreign organisms, release antimicrobial peptides, secrete molecules that attract other immune cells to areas of infection, and present antigens to lymphocytes (64).

Activated macrophages release stereotypical profiles of cytokines and biologically active molecules such as NO, TNF-α, IL-6, and IL-1 (64). Depletion of macrophages from sites of inflammation prevents the elaboration of these molecules (65, 66). These molecules increase the production of acute-phase proteins. Increased TNF-α signaling mediates increased PAI-1 production in acute inflammation and in obesity (67). Increased IL-6 signaling induces the expression of C-reactive protein and haptoglobin in liver (68).

The strong relationship between adipose tissue macrophage content and indicators of adiposity provides a mechanism for the increased adipose tissue production of proinflammatory molecules and acute-phase proteins associated with obesity. Adipose tissue produces several proinflammatory, procoagulant, and acute-phase molecules in direct proportion to adiposity. Among these molecules, TNF-α, IL-6, PAI-1, NO, factor VII, and MCP-1 have been implicated in the development of adverse pathophysiological phenotypes associated with obesity (25, 69). For example, iNOS and TNF-α are required for the development of obesity-induced insulin resistance in mice (21, 29). TNF-α and IL-6 also increase lipolysis and have been implicated in the hypertriglyceridemia and increased serum FFA levels associated with obesity (31, 32). The increased production of PAI-1 and factor VII has been implicated in the development of coagulation and fibrinolytic abnormalities characteristic of obesity (28, 70). Macrophage accumulation in proportion to adipocyte size may increase the adipose tissue production of these proinflammatory and acute-phase molecules and thereby contribute to the pathophysiological consequences of obesity.

Skeletal muscle tissue also produces increased amounts of iNOS and TNF-α in obese compared with lean rodents and humans (21, 71). Both NO and TNF-α decrease insulin-stimulated glucose uptake in muscle (72, 73). Our results indicate that the percentage of macrophages in the adipose tissue that surrounds and infiltrates the extensor digitalis longus muscle is increased in obese mice compared with lean mice. The production of iNOS and TNF-α by these macrophages may contribute to the decreased insulin sensitivity of muscle that is characteristic of obesity.

Our data in humans and mice show that adipocyte size is a strong predictor of the percentage of macrophages in adipose tissue (Figure 3e). Adipose tissue mass is the product of cell number and volume. Adipocyte volume is highly correlated with indicators of systemic insulin resistance, dyslipidemia, and risk for developing type 2 diabetes (74–77). Weight reduction is accompanied by decreased adipocyte volume and the reduction of these metabolic phenotypes (78, 79). Mechanisms have been proposed by which adipocyte hypertrophy may perturb adipocyte function in a cell-autonomous fashion and thereby influence systemic glucose and lipid metabolism (80–82). The close relationship between adipocyte size and the abundance of macrophages in adipose tissue suggests that the influence of adipocyte size on adipocyte function may be conveyed through a paracrine pathway involving adipose tissue macrophages.

Adipose tissue macrophages may be a target for the thiazolidinedione (TZD) class of antidiabetic drugs. TZDs increase systemic insulin sensitivity and adipose tissue triglyceride storage while decreasing adipose tissue fatty acid efflux (83). The mechanisms by which TZDs exert these effects on glucose and lipid metabolism are not completely defined, though many of their actions appear to be mediated through activation of the nuclear hormone receptor PPAR-γ. Adipocytes express high levels of PPAR-γ, and TZDs promote adipocyte differentiation, prevent fatty acid release, and stimulate adiponectin production, suggesting that adipocytes are an important target for TZD action (84–86). Macrophages also express high levels of PPAR-γ. TZDs and other PPAR-γ agonists suppress macrophage production of TNF-α, IL-6, NO, and IL-1β induced by LPS and IFN-γ (87–90). The action of TZDs on adipose tissue macrophages may decrease local production and concentrations of proinflammatory factors and thereby contribute to their physiologically beneficial effects on glucose and lipid metabolism.

The correlation of adipose tissue macrophage content with adiposity may affect the interpretation of results obtained from mice in which transgene expression is driven by the aP2 promoter. To target expression and to delete genes specifically in adipocytes, investigators have often used the aP2 promoter (91). The *aP2* gene is highly expressed in differentiated adipocytes but has recently been shown to be expressed by macrophages as well (52). Our findings suggest that data obtained from aP2 transgenics will need to be carefully analyzed to distinguish between effects occurring primarily in adipocytes or macrophages.

Our data also suggest that the increased accumulation of macrophages in adipose tissue of the obese is due to an influx of bone marrow–derived precursors into adipose tissue and their subsequent differentiation into mature F4/80-expressing macrophages. A recent report showed that adipose tissue production of MCP-1 — a chemoattractant specific for monocytes and macrophages — is increased in leptin-deficient mice compared with lean mice (25, 92, 93). Our data indicate that the expression of this chemokine and several others are significantly and positively correlated with body mass in the perigonadal adipose tissue of mice (Supplemental Table 1, http://www.jci.org/cgi/content/full/112/12/1796/DC1). Adipocytes also produce CSF-1, the primary regulator of macrophage differentiation and survival (94). Therefore, with increasing adiposity, adipose tissue may release signals such as MCP-1, causing increased monocyte influx. The production of CSF-1 by adipocytes may then create a permissive microenvironment for these monocytes to differentiate and survive as mature adipose tissue macrophages.

Acknowledgments

We thank E. Richard Stanley for the gift of FVB/NJ *Csf1*$^{op/op}$ mice. This work was supported by grants from the NIH NIDDK (K08 DK-59960 and R01 DK-66525 to A.W. Ferrante, Jr.; R01 DK-052431 to R.L. Leibel), the Fawcett Foundation, and the Russell Berrie Foundation. We thank Domenico Accili, E. Richard Stanley, and Yiying Zhang for their comments and suggestions.

1. Tai, E.S., Lau, T.N., Ho, S.C., Fok, A.C., and Tan, C.E. 2000. Body fat distribution and cardiovascular risk in normal weight women. Associations with insulin resistance, lipids and plasma leptin. *Int. J. Obes. Relat. Metab. Disord.* **24**:751–757.
2. Messerli, F.H., et al. 1981. Obesity and essential hypertension. Hemodynamics, intravascular volume, sodium excretion, and plasma renin activity. *Arch. Intern. Med.* **141**:81–85.
3. Liuzzi, A., et al. 1999. Serum leptin concentration in moderate and severe obesity: relationship with clinical, anthropometric and metabolic factors. *Int. J. Obes. Relat. Metab. Disord.* **23**:1066–1073.
4. Janssen, I., Katzmarzyk, P.T., and Ross, R. 2002. Body mass index, waist circumference, and health risk: evidence in support of current National Institutes of Health guidelines. *Arch. Intern. Med.* **162**:2074–2079.
5. Stolk, R.P., Meijer, R., Mali, W.P., Grobbee, D.E., and van der Graaf, Y. 2003. Ultrasound measurements of intraabdominal fat estimate the metabolic syndrome better than do measurements of waist circumference. *Am. J. Clin. Nutr.* **77**:857–860.
6. DiPietro, L., Katz, L.D., and Nadel, E.R. 1999. Excess abdominal adiposity remains correlated with altered lipid concentrations in healthy older women. *Int. J. Obes. Relat. Metab. Disord.* **23**:432–436.
7. Hubert, H.B., Feinleib, M., McNamara, P.M., and Castelli, W.P. 1983. Obesity as an independent risk factor for cardiovascular disease: a 26-year follow-up of participants in the Framingham Heart Study. *Circulation.* **67**:968–977.
8. Kurth, T., et al. 2002. Body mass index and the risk of stroke in men. *Arch. Intern. Med.* **162**:2557–2562.
9. Calle, E.E., Rodriguez, C., Walker-Thurmond, K., and Thun, M.J. 2003. Overweight, obesity, and mortality from cancer in a prospectively studied cohort of U.S. adults. *N. Engl. J. Med.* **348**:1625–1638.
10. Rosenbaum, M., and Leibel, R.L. 1999. The role of leptin in human physiology. *N. Engl. J. Med.* **341**:913–915.
11. Maffei, M., et al. 1995. Increased expression in adipocytes of ob RNA in mice with lesions of the hypothalamus and with mutations at the db locus. *Proc. Natl. Acad. Sci. U. S. A.* **92**:6957–6960.
12. Frederich, R.C., et al. 1995. Expression of ob mRNA and its encoded protein in rodents. Impact of nutrition and obesity. *J. Clin. Invest.* **96**:1658–1663.
13. Zhang, Y., Guo, K.Y., Diaz, P.A., Heo, M., and Leibel, R.L. 2002. Determinants of leptin gene expression in fat depots of lean mice. *Am. J. Physiol. Regul. Integr. Comp. Physiol.* **282**:R226–R234.
14. Bodary, P.F., Westrick, R.J., Wickenheiser, K.J., Shen, Y., and Eitzman, D.T. 2002. Effect of leptin on arterial thrombosis following vascular injury in mice. *JAMA.* **287**:1706–1709.
15. Arita, Y., et al. 1999. Paradoxical decrease of an adipose-specific protein, adiponectin, in obesity. *Biochem. Biophys. Res. Commun.* **257**:79–83.
16. Combs, T.P., Berg, A.H., Obici, S., Scherer, P.E., and Rossetti, L. 2001. Endogenous glucose production is inhibited by the adipose-derived protein Acrp30. *J. Clin. Invest.* **108**:1875–1881. doi:10.1172/JCI200114120.
17. Tomas, E., et al. 2002. Enhanced muscle fat oxidation and glucose transport by ACRP30 globular domain: acetyl-CoA carboxylase inhibition and AMP-activated protein kinase activation. *Proc. Natl. Acad. Sci. U. S. A.* **99**:16309–16313.
18. Hotamisligil, G.S., Shargill, N.S., and Spiegelman, B.M. 1993. Adipose expression of tumor necrosis factor-alpha: direct role in obesity-linked insulin resistance. *Science.* **259**:87–91.
19. Fried, S.K., Bunkin, D.A., and Greenberg, A.S. 1998. Omental and subcutaneous adipose tissues of obese subjects release interleukin-6: depot difference and regulation by glucocorticoid. *J. Clin. Endocrinol. Metab.* **83**:847–850.
20. Vgontzas, A.N., et al. 1997. Elevation of plasma cytokines in disorders of excessive daytime sleepiness: role of sleep disturbance and obesity. *J. Clin. Endocrinol. Metab.* **82**:1313–1316.
21. Perreault, M., and Marette, A. 2001. Targeted disruption of inducible nitric oxide synthase protects against obesity-linked insulin resistance in muscle. *Nat. Med.* **7**:1138–1143.
22. Samad, F., Yamamoto, K., Pandey, M., and Loskutoff, D.J. 1997. Elevated expression of transforming growth factor-beta in adipose tissue from obese mice. *Mol. Med.* **3**:37–48.
23. Visser, M., Bouter, L.M., McQuillan, G.M., Wener, M.H., and Harris, T.B. 1999. Elevated C-reactive protein levels in overweight and obese adults. *JAMA.* **282**:2131–2135.
24. Weyer, C., et al. 2002. Humoral markers of inflammation and endothelial dysfunction in relation to adiposity and in vivo insulin action in Pima Indians. *Atherosclerosis.* **161**:233–242.
25. Sartipy, P., and Loskutoff, D.J. 2003. Monocyte chemoattractant protein 1 in obesity and insulin resistance. *Proc. Natl. Acad. Sci. U. S. A.* **100**:7265–7270.
26. Samad, F., Yamamoto, K., and Loskutoff, D.J. 1996. Distribution and regulation of plasminogen activator inhibitor-1 in murine adipose tissue in vivo. Induction by tumor necrosis factor-alpha and lipopolysaccharide. *J. Clin. Invest.* **97**:37–46.
27. Samad, F., Pandey, M., and Loskutoff, D.J. 1998. Tissue factor gene expression in the adipose tissues of obese mice. *Proc. Natl. Acad. Sci. U. S. A.* **95**:7591–7596.
28. De Pergola, G., and Pannacciulli, N. 2002. Coagulation and fibrinolysis abnormalities in obesity. *J. Endocrinol. Invest.* **25**:899–904.
29. Uysal, K.T., Wiesbrock, S.M., Marino, M.W., and Hotamisligil, G.S. 1997. Protection from obesity-induced insulin resistance in mice lacking TNF-alpha function. *Nature.* **389**:610–614.
30. Hotamisligil, G.S., Murray, D.L., Choy, L.N., and Spiegelman, B.M. 1994. Tumor necrosis factor alpha inhibits signaling from the insulin receptor. *Proc. Natl. Acad. Sci. U. S. A.* **91**:4854–4858.
31. Zhang, H.H., Halbleib, M., Ahmad, F., Manganiello, V.C., and Greenberg, A.S. 2002. Tumor necrosis factor-alpha stimulates lipolysis in differentiated human adipocytes through activation of extracellular signal-related kinase and elevation of intracellular cAMP. *Diabetes.* **51**:2929–2935.
32. Nonogaki, K., et al. 1995. Interleukin-6 stimulates hepatic triglyceride secretion in rats. *Endocrinology.* **136**:2143–2149.
33. Ross, S.E., et al. 2002. Microarray analyses during adipogenesis: understanding the effects of Wnt signaling on adipogenesis and the roles of liver X receptor alpha in adipocyte metabolism. *Mol. Cell. Biol.* **22**:5989–5999.
34. Fain, J.N., Cheema, P.S., Bahouth, S.W., and Lloyd Hiler, M. 2003. Resistin release by human adipose tissue explants in primary culture. *Biochem. Biophys. Res. Commun.* **300**:674–678.
35. Bultman, S.J., Michaud, E.J., and Woychik, R.P. 1992. Molecular characterization of the mouse agouti locus. *Cell.* **71**:1195–1204.
36. Leibel, R.L., Chung, W.K., and Chua, S.C., Jr. 1997. The molecular genetics of rodent single gene obesities. *J. Biol. Chem.* **272**:31937–31940.
37. Robinson, S.W., Dinulescu, D.M., and Cone, R.D. 2000. Genetic models of obesity and energy balance in the mouse. *Annu. Rev. Genet.* **34**:687–745.
38. Rosenbaum, M., et al. 2003. Effects of experimental weight perturbation on skeletal muscle work efficiency in human subjects. *Am. J. Physiol. Regul. Integr. Comp. Physiol.* **285**:R183–R192.
39. Rosenbaum, M., Murphy, E.M., Heymsfield, S.B., Matthews, D.E., and Leibel, R.L. 2002. Low dose leptin administration reverses effects of sustained weight-reduction on energy expenditure and circulating concentrations of thyroid hormones. *J. Clin. Endocrinol. Metab.* **87**:2391–2394.
40. Leibel, R.L., Rosenbaum, M., and Hirsch, J. 1995. Changes in energy expenditure resulting from altered body weight. *N. Engl. J. Med.* **332**:621–628.
41. Benjamini, Y., and Hochberg, Y. 1995. Controlling the false discovery rate: a practical and powerful approach to multiple testing. *Journal of the Royal Statistical Society, Series B.* **57**:289–300.
42. Slonim, D.K. 2002. From patterns to pathways: gene expression data analysis comes of age. *Nat. Genet.* **32**(Suppl.):502–508.
43. Cecchini, M.G., et al. 1994. Role of colony stimulating factor-1 in the establishment and regulation of tissue macrophages during postnatal development of the mouse. *Development.* **120**:1357–1372.
44. Vandesompele, J., et al. 2002. Accurate normalization of real-time quantitative RT-PCR data by geometric averaging of multiple internal control genes. *Genome Biol.* **3**:RESEARCH0034.
45. Rosen, S., and Skaletsky, H. 2000. Primer3 on the WWW for general users and for biologist programmers. In *Bioinformatics methods and protocols: methods in molecular biology*. S. Misener and S.A. Krawetz, editors. Humana Press. Totowa, New Jersey, USA. 365–386.
46. Snedecor, G.W., and Cochran, W.G. 1967. *Statistical methods*. Iowa State University Press. Ames, Iowa, USA. 172–198.
47. Prieditis, H., and Adamson, I.Y. 1996. Alveolar macrophage kinetics and multinucleated giant cell formation after lung injury. *J. Leukoc. Biol.* **59**:534–538.
48. Toyosaki-Maeda, T., et al. 2001. Differentiation of monocytes into multinucleated giant bone-resorbing cells: two-step differentiation induced by nurse-like cells and cytokines. *Arthritis Res.* **3**:306–310.
49. Athanasou, N.A., and Quinn, J. 1990. Immunophenotypic differences between osteoclasts and macrophage polykaryons: immunohistological distinction and implications for osteoclast ontogeny and function. *J. Clin. Pathol.* **43**:997–1003.
50. Endemann, G., et al. 1993. CD36 is a receptor for oxidized low density lipoprotein. *J. Biol. Chem.* **268**:11811–11816.
51. Lee, C.H., and Evans, R.M. 2002. Peroxisome proliferator-activated receptor-gamma in macrophage lipid homeostasis. *Trends Endocrinol. Metab.* **13**:331–335.

52. Makowski, L., et al. 2001. Lack of macrophage fatty-acid-binding protein aP2 protects mice deficient in apolipoprotein E against atherosclerosis. *Nat. Med.* **7**:699–705.
53. Cousin, B., et al. 1999. A role for preadipocytes as macrophage-like cells. *FASEB J.* **13**:305–312.
54. Wiktor-Jedrzejczak, W., et al. 1990. Total absence of colony-stimulating factor 1 in the macrophage-deficient osteopetrotic (op/op) mouse. *Proc. Natl. Acad. Sci. U. S. A.* **87**:4828–4832.
55. Yoshida, H., et al. 1990. The murine mutation osteopetrosis is in the coding region of the macrophage colony stimulating factor gene. *Nature.* **345**:442–444.
56. Stanley, E.R., et al. 1997. Biology and action of colony-stimulating factor-1. *Mol. Reprod. Dev.* **46**:4–10.
57. Dai, X.M., Zong, X.H., Sylvestre, V., and Stanley, E.R. 2003. Incomplete restoration of colony stimulating factor-1 (CSF-1) function in CSF-1–deficient Csf1op/Csf1op mice by transgenic expression of cell surface CSF-1. *Blood.* doi:10.1182/blood-2003-08-2739.
58. Kullo, I.J., Hensrud, D.D., and Allison, T.G. 2002. Comparison of numbers of circulating blood monocytes in men grouped by body mass index (<25, 25 to <30, > or = 30). *Am. J. Cardiol.* **89**:1441–1443.
59. Soukas, A., Cohen, P., Socci, N.D., and Friedman, J.M. 2000. Leptin-specific patterns of gene expression in white adipose tissue. *Genes Dev.* **14**:963–980.
60. Cousin, B., Andre, M., Casteilla, L., and Penicaud, L. 2001. Altered macrophage-like functions of preadipocytes in inflammation and genetic obesity. *J. Cell. Physiol.* **186**:380–386.
61. Gordon, S. 1995. The macrophage. *Bioessays.* **17**:977–986.
62. Bornstein, S.R., et al. 2000. Immunohistochemical and ultrastructural localization of leptin and leptin receptor in human white adipose tissue and differentiating human adipose cells in primary culture. *Diabetes.* **49**:532–538.
63. Charriere, G., et al. 2003. Preadipocyte conversion to macrophage. Evidence of plasticity. *J. Biol. Chem.* **278**:9850–9855.
64. Gordon, S. 1998. The role of the macrophage in immune regulation. *Res. Immunol.* **149**:685–688.
65. Torres, P.F., et al. 1999. Changes in cytokine mRNA levels in experimental corneal allografts after local clodronate-liposome treatment. *Invest. Ophthalmol. Vis. Sci.* **40**:3194–3201.
66. Koay, M.A., et al. 2002. Macrophages are necessary for maximal nuclear factor-kappa B activation in response to endotoxin. *Am. J. Respir. Cell Mol. Biol.* **26**:572–578.
67. Pandey, M., Tuncman, G., Hotamisligil, G.S., and Samad, F. 2003. Divergent roles for p55 and p75 TNF-alpha receptors in the induction of plasminogen activator inhibitor-1. *Am. J. Pathol.* **162**:933–941.
68. Morrone, G., et al. 1988. Recombinant interleukin 6 regulates the transcriptional activation of a set of human acute phase genes. *J. Biol. Chem.* **263**:12554–12558.
69. Pickup, J.C., and Crook, M.A. 1998. Is type II diabetes mellitus a disease of the innate immune system? *Diabetologia.* **41**:1241–1248.
70. Rissanen, P., Vahtera, E., Krusius, T., Uusitupa, M., and Rissanen, A. 2001. Weight change and blood coagulability and fibrinolysis in healthy obese women. *Int. J. Obes. Relat. Metab. Disord.* **25**:212–218.
71. Saghizadeh, M., Ong, J.M., Garvey, W.T., Henry, R.R., and Kern, P.A. 1996. The expression of TNF alpha by human muscle. Relationship to insulin resistance. *J. Clin. Invest.* **97**:1111–1116.
72. Kapur, S., Bedar, S., Marcotte, B., Cote, C.H., and Marette, A. 1997. Expression of nitric oxide synthase in skeletal muscle: a novel role for nitric oxide as a modulator of insulin action. *Diabetes.* **46**:1691–1700.
73. Youd, J.M., Rattigan, S., and Clark, M.G. 2000. Acute impairment of insulin-mediated capillary recruitment and glucose uptake in rat skeletal muscle in vivo by TNF-alpha. *Diabetes.* **49**:1904–1909.
74. Schneider, B.S., Faust, I.M., Hemmes, R., and Hirsch, J. 1981. Effects of altered adipose tissue morphology on plasma insulin levels in the rat. *Am. J. Physiol.* **240**:E358–E362.
75. Weyer, C., et al. 2001. Subcutaneous abdominal adipocyte size, a predictor of type 2 diabetes, is linked to chromosome 1q21—q23 and is associated with a common polymorphism in LMNA in Pima Indians. *Mol. Genet. Metab.* **72**:231–238.
76. Weyer, C., Foley, J.E., Bogardus, C., Tataranni, P.A., and Pratley, R.E. 2000. Enlarged subcutaneous abdominal adipocyte size, but not obesity itself, predicts type II diabetes independent of insulin resistance. *Diabetologia.* **43**:1498–1506.
77. Stern, J.S., Batchelor, B.R., Hollander, N., Cohn, C.K., and Hirsch, J. 1972. Adipose-cell size and immunoreactive insulin levels in obese and normal-weight adults. *Lancet.* **2**:948–951.
78. Jimenez, J., Zuniga-Guajardo, S., Zinman, B., and Angel, A. 1987. Effects of weight loss in massive obesity on insulin and C-peptide dynamics: sequential changes in insulin production, clearance, and sensitivity. *J. Clin. Endocrinol. Metab.* **64**:661–668.
79. Kral, J.G., Bjorntorp, P., Schersten, T., and Sjostrom, L. 1977. Body composition and adipose tissue cellularity before and after jejuno-ileostomy in severely obese subjects. *Eur. J. Clin. Invest.* **7**:413–419.
80. Salans, L.B., and Dougherty, J.W. 1971. The effect of insulin upon glucose metabolism by adipose cells of different size. Influence of cell lipid and protein content, age, and nutritional state. *J. Clin. Invest.* **50**:1399–1410.
81. Hissin, P.J., et al. 1982. Mechanism of insulin-resistant glucose transport activity in the enlarged adipose cell of the aged, obese rat. *J. Clin. Invest.* **70**:780–790.
82. Le Lay, S., et al. 2001. Cholesterol, a cell size-dependent signal that regulates glucose metabolism and gene expression in adipocytes. *J. Biol. Chem.* **276**:16904–16910.
83. Oakes, N.D., Thalen, P.G., Jacinto, S.M., and Ljung, B. 2001. Thiazolidinediones increase plasma-adipose tissue FFA exchange capacity and enhance insulin-mediated control of systemic FFA availability. *Diabetes.* **50**:1158–1165.
84. Maeda, N., et al. 2001. PPARgamma ligands increase expression and plasma concentrations of adiponectin, an adipose-derived protein. *Diabetes.* **50**:2094–2099.
85. Tordjman, J., et al. 2003. Thiazolidinediones block fatty acid release by inducing glyceroneogenesis in fat cells. *J. Biol. Chem.* **278**:18785–18790.
86. Guan, H.P., et al. 2002. A futile metabolic cycle activated in adipocytes by antidiabetic agents. *Nat. Med.* **8**:1122–1128.
87. Jiang, C., Ting, A.T., and Seed, B. 1998. PPAR-gamma agonists inhibit production of monocyte inflammatory cytokines. *Nature.* **391**:82–86.
88. Chawla, A., et al. 2001. PPAR-gamma dependent and independent effects on macrophage-gene expression in lipid metabolism and inflammation. *Nat. Med.* **7**:48–52.
89. Alleva, D.G., et al. 2002. Regulation of murine macrophage proinflammatory and anti-inflammatory cytokines by ligands for peroxisome proliferator-activated receptor-gamma: counter-regulatory activity by IFN-gamma. *J. Leukoc. Biol.* **71**:677–685.
90. Ricote, M., Li, A.C., Willson, T.M., Kelly, C.J., and Glass, C.K. 1998. The peroxisome proliferator-activated receptor-gamma is a negative regulator of macrophage activation. *Nature.* **391**:79–82.
91. Ross, S.R., Graves, R.A., and Spiegelman, B.M. 1993. Targeted expression of a toxin gene to adipose tissue: transgenic mice resistant to obesity. *Genes Dev.* **7**:1318–1324.
92. Boring, L., et al. 1997. Impaired monocyte migration and reduced type 1 (Th1) cytokine responses in C-C chemokine receptor 2 knockout mice. *J. Clin. Invest.* **100**:2552–2561.
93. Lu, B., et al. 1998. Abnormalities in monocyte recruitment and cytokine expression in monocyte chemoattractant protein 1-deficient mice. *J. Exp. Med.* **187**:601–608.
94. Levine, J.A., Jensen, M.D., Eberhardt, N.L., and O'Brien, T. 1998. Adipocyte macrophage colony-stimulating factor is a mediator of adipose tissue growth. *J. Clin. Invest.* **101**:1557–1564.